Available online at www.sciencedirect.com
SCIENCE DIRECT®
Journal of Nuclear Materials 335 (2004) 286–292
journal of nuclear materials
www.elsevier.com/locate/jnucmat

Turbulent heat mixing of a heavy liquid metal flow within the MEGAPIE window geometry: The heated jet experiments

M. Daubner, A. Batta, F. Fellmoser, C.-H. Lefhalm, K.-J. Mack, R. Stieglitz *

Institute for Nuclear and Energy Technologies (IKET), Forschungszentrum Karlsruhe, P.O. Box 3640, D-76021 Karlsruhe, Germany

Abstract

The use of heavy liquid metals (HLM) serving both as coolant and as spallation source facilitates simple beam window geometries. An adequate cooling of the beam window requires a conditioning of the flow. Within the MEGAPIE window this is realized in a cylindrically shaped geometry, in which the main flow is guided in an annular gap downwards and then u-turned close to a hemispherical shell into a riser tube. In order to avoid stagnating fluid domains leading to unacceptably high window temperatures a jet flow is injected in direction of the lower shell. In this study the turbulent mixing of hot jet into a cold main flow is investigated both experimentally and numerically for the MEGAPIE geometry on a 1:1 scale. The experiments have been conducted in the Karlsruhe Lead Laboratory (KALLA). In parallel a numerical simulation has been performed. Close to the technically most interesting positions in the lower shell, a reasonably good agreement between numerical and experimental data has been found. Here, a sufficient description of the turbulent heat transfer in a lead–bismuth flow was obtained. However, as the flow proceeds downstream not only qualitative but quantitative differences appear, which have to be analyzed in more detail in the future.

1. Introduction

Beam windows facing the proton beam of an accelerator have to withstand high heat fluxes of up to 140 W/cm^2. Although this is only a small part of the total proton beam power (~1%), it represents one of the most critical technical issues to be solved for a liquid metal cooled system. In order to minimize the heat release in the structural material these beam windows are relatively thin like the MEGAPIE beam window, which is made of a 1–2 mm thin T91 (9Cr–1Mo VNb) martensitic steel shell. Besides this material issue an adequate heat transfer from the wall towards the coolant and neutron producing heavy liquid metal PbBi has to be ensured for all beam states appearing during operation. Thus, only the detailed knowledge of the convective–diffusive heat transport phenomena in turbulent heavy liquid metal flows enables an adequate design of such a beam window. Due to the low molecular Prandtl number of liquid metals being of the order $O(10^{-1}$–$10^{-2})$ a decoupling of kinematic and thermal transfer processes appears, which is often not sufficiently treated in commercial computational fluid dynamics (CFD) codes.

The simulation of heat production scenarios as they appear in HLM cooled beam windows are hardly feasi-

* Corresponding author. Tel.: +49 7247 82 3462; fax: +49 7247 3462.
E-mail address: robert.stieglitz@iket.fzk.de (R. Stieglitz).

0022-3115/$ - see front matter © 2004 Elsevier B.V. All rights reserved.
doi:10.1016/j.jnucmat.2004.07.029

ble out of pile, because three different turbulent heat transfer phenomena occur simultaneously in the vicinity of the hemispherical, shell as depicted in Fig. 1. These are:

1. Turbulent heat transfer from a highly heat loaded surface.
2. Cooling of the stagnation point of the shell via an imposed secondary jet flow (turbulent mixing phenomenon).
3. Internal heat generation (volumetric heating) by the spallation reactions.

Assuming prototypical velocities in the beam window hydraulic Reynolds numbers Re of $O(10^5)$ are obtained. This yields for the first two problems that the temperature can be considered to the leading order acting as a passive scalar. Hence, an experimental simulation is possible, the latter one is almost impracticable out of pile. The solution strategy for the MEGAPIE window is to perform two benchmark experiments, with which the numerical CFD tools are validated. Finally, the verified package is applied to the third phenomenon [1,2]. We concentrate our discussion in this article on the turbulent mixing of a hot lead–bismuth jet into a cold main flow in the MEGAPIE configuration.

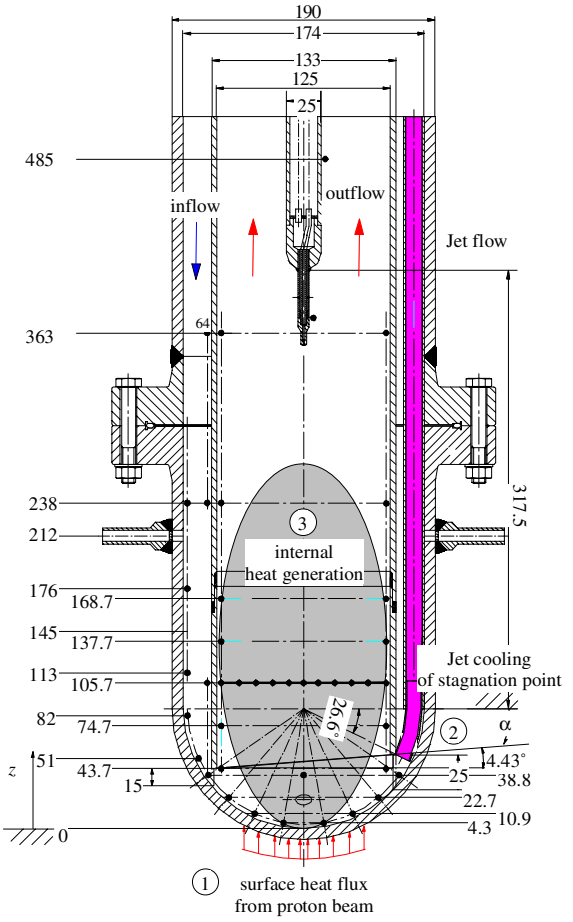

Fig. 1. Drawing of the beam window and description of the heat transfer problems. The numbers indicate thermocouple positions. Introduction of the coordinate system.

2. Experimental set-up of the heated jet experiment

Within the KALLA laboratory the lower part of the MEGAPIE beam window has been fabricated and instrumented in 1:1 geometric scale using stainless steel, see Fig. 1. The main flow is entering the module in the upper collector and guided via steel vanes into a flow straightener made of 24 tubes with an inner diameter of 15 mm and length of 150 mm in order to ensure a fully developed turbulent flow in a height of $z = 1625$ mm. The centerline of the jet channel enters the annular gap at $z = 1683$ mm. The gap adapted geometry of the jet pipe has rectangular edges, is made of 2 mm thick steel sheets, and has at its centerline an inner orifice of 100×10 mm. At $z = 107$ mm, the nozzle with an inner orifice of 20×10 mm is welded to the jet duct, as illustrated in Fig. 2. The centerline orifice is located at $z = 51$ mm and its inner tube contacts the slanted riser tube at the position of maximum inclination.

In the lower shell, 18 0.5-mm thick thermocouples (TC's) are embedded at a distance of 3 mm from the wall in the shell in the direction of the jet flow and perpendicular to it. The merging main and jet flows are directed upwards in a riser tube, which is inclined in order to generate a secondary swirl flow superposed on the axial transport velocity. The distance of the riser tube to the shell is 15 mm at $\phi = 180°$ and 25 mm at $\phi = 0°$. Within the riser tube thermocouples are embedded close to the fluid-wall interface and a thermocouple rake consisting of 17 thermocouples in the planes $\phi = 0°$ and $\phi = 90°$. The flow is facing the instrumentation rod at $z = 349$ mm. At $z = 404.5$ mm, the instrumentation rod is spherically shaped to its final outer diameter of 25 mm. Finally, the fluid is leaving the module at $z = 2340$ mm and $\phi = 90°$ towards the THEADES loop.

Both main flow and jet flow are fed by one pump. The different flow rates are established using regulation valves in the individual branches. Both flow rates are monitored simultaneously using six flow meters with different measurement principles ensuring an accuracy after calibration of ±2% for the flow rate. The jet flow is heated before entering the module using electrical resistance heaters. The heating power is continuously recorded and regulated, so that the temperature at the jet flow inlet can be set to a constant value. The test section is insulated with a 160 mm thick rock wool layer

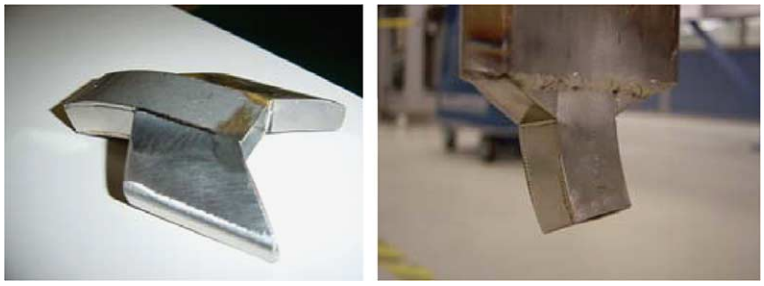

Fig. 2. Photograph of the nozzle.

($\lambda = 0.043$ W/(mK)). As a reference case for the experiment, a heating power of 31 kW has been chosen with a flow rate of $Q_{main} = 18$ m^3/h and $Q_{jet} = 1.2$ m^3/h at an average inlet temperature of the main flow of $T_{in} = 300$ °C.

3. Numerical simulation

The heated jet experiment has been simulated using the commercially available CFD code CFX. Since a modeling of the whole geometry with an adequate resolution of the boundary layers and the structures exceeds the available computer resources the numerical simulation represents the geometry on a 1:1 scale up to a height of $z = 890$ mm, for which cylinder symmetry is assumed and symmetry conditions are applied in the plane $\phi = 0°$. The structured grid generated consists of 1.2×10^6 cells and has been chosen in such a manner, that a high resolution near the walls in terms of low y^+ values has been achieved.

The simulation includes heat conduction processes within the steel structures confining the flow. In order to limit the computational effort the outer thick steel wall and the instrumentation rod have not been integrated into the simulation. The first, because the heat losses to the ambient where found to be very small in the experiment, and the second, because of its complexity of grid generation. At the outer fluid domain confining wall interface the non-slip condition and a zero heat flux has been applied. Although the latter condition is problematic, because the specific heat conductivity of the steel is comparable to that of the eutectic lead–bismuth, it reduces the computational effort considerably. Of crucial importance are the inlet conditions at $z = 890$ mm. Regarding the velocity a fully developed profile has been used, being aware that the developing length is only about 20 characteristic lengths in terms of the hydraulic diameter of the gap. Estimates in the literature [3] show that this yields errors of less than 3% for the turbulent kinetic energy k and the velocity profile. The choice of a reduced geometrical length, however, causes significant errors in the temperature field, because a considerable amount of the thermal energy of the jet has been already transferred to the gap flow before entering the simulation domain (i.e. 1683 mm $< z <$ 890 mm).

Within the simulation the SST turbulence model has been used. The SST model combines the advantages of the k–ε model with the ones of the k–ω model and takes advantage of the fact that for use of the k–ω model in the near wall region an analytical solution for the viscous sublayer is known for small y^+ values, see Wilcox [3]. The matching of the k–ω model close to all walls to the k–ε model in the rest of the fluid domain is performed by means of blending functions [4]. The temperature wall function is modeled using the formulation proposed by Kader [5]. Regarding the advection terms in the turbulent simulation a second order differencing scheme has been used.

The main dimensionless groups entering the description of the problem are the hydraulic Reynolds number, the kinetic Froude number, the densimetric Froud, which are defined as:

$$Re = \frac{u_0 \cdot d_h}{\nu}; \quad Fr_{kin} = \frac{(u_{jet}^2 - u_{main}^2)}{g \cdot d_{h,jet}};$$
$$Fr_{kin} = \frac{\rho_{main}(u_{jet}^2 - u_{main}^2)}{(\rho_{main} - \rho_{jet}) g \cdot d_{h,jet}}, \tag{1}$$

where u_0 denotes the mean velocity, d_h the hydraulic diameter, g the gravity constant and the liquid properties are the specific viscosity ν and the density ρ, which may be taken from [6].

Both hydraulic Reynolds numbers, the one of the jet and that of the main flow are for the defined reference case of $O(10^5)$ indicating a fully turbulent flow and a mainly inertia driven system. The kinetic Froude number, which is a measure of the relative momentum between both streams is relatively small, i.e. $Fr_{kin} = 19.28$. This relatively small value yields that the additional turbulent shear produced by the jet is weak and thus the position of the nozzle and its impact on the temperature distribution on the lower shell is sensitive. The corresponding densimetric Froude number assuming a nozzle exit temperature of $T_{nozzle} = 350$ °C is of $O(10^3)$

and hence clearly in the inertial range of co-arranged jets, see [7]. The transformation of the thermal energy into kinetic energy in inertial jets starts is most pronounced for $l/d_{\mathrm{h,jet}} \gg 10$ as discussed in [8], where l is the distance from the nozzle exit. Thus, the additional impact of buoyancy effects is mainly occurring downstream in the riser rather than close to the shell. As a consequence, the numerical simulation first concentrated on a calculation neglecting buoyancy and using constant specific fluid properties. Future simulations will integrate the omitted issues.

In Fig. 3(a) and (b) the calculated velocity vectors in the r–z-plane ($\phi = 0°$ and $\phi = 90°$) are shown for the defined reference conditions.

The main flow in the annular gap far from the window is fully developed in the r–z-plane expressed by a slug flow velocity profile except for the region of the jet duct. As the main flow approaches the window region, the cross section is continuously decreasing and the main flow is accelerated (0, see Fig. 6(b)). The discontinuity of the geometry at the transition of the downwards oriented gap flow into the upwards directed riser flow leads to a flow separation. This flow separation is expressed by the formation of a recirculation zone (1) at the beginning of the riser tube, see Fig. 3(b). Adjacent to the recirculation zone close to the center line, a jet (2) is formed with velocities being about 2.5 times higher than the mean velocity. In the lower part of the shell, a second recirculation domain (3) establishes itself with extremely low velocities. Those small velocities would lead in the real MEGAPIE case to unacceptably high temperatures. The plane, $\phi = 90°$, is hardly affected by the jet flow arising from the 20×10 mm nozzle. In the plane $\phi = 0°$, the jet flow is superimposed on the main flow. As the jet exits the nozzle it forces by its momentum a large portion of the fluid towards the opposite side of the riser tube (5). A part of the jet flow also impinges upon the lower hemispherical shell (6). Nevertheless, close to the centerline in the lower part of the shell at $r = z = 0$, the fluid velocity still remains small. The momentum transfer from the nozzle to the main flow creates a third recirculation zone in the $\phi = 0°$ plane in a large flow domain (4).

Since the heat transfer in the heated jet experiment is mainly governed by momentum exchange, the flow pattern is reflected also in the temperature field, which is depicted in Fig. 4(a) and (b) in the r–z-plane ($\phi = 0°$ and $\phi = 90°$). In Fig. 4(a) the heat loss of the jet flow towards the main flow is easily visible. Within the simulation, a temperature decrease of about 9.6 °C per meter of the jet duct has been obtained. Directly at the jet nozzle the simulation reveals a value of 342 °C, whereas the experiment shows 334 °C. The reason for this deviation is that the simulation has been only performed up to $z = 890$ mm and that the heat conduction in the outer steel wall has been neglected. Extrapolating the heat losses to the real geometry the temperature directly at the nozzle exit would be 333.8 °C without considering the heat losses to the ambient environment.

As the jet exits the nozzle, the temperatures close to the shell (TC 3, 4, 5) at the fluid wall interface experience do not a drastic elevation, since most of the heat is transported by the momentum of the jet towards the central core in the riser tube. The impact of the jet on the temperature distribution in the lower part of the shell close to $r = z = 0$ is small (TC 3, 4). The temperature rise in the centerline (TC 6 and 7, see Fig. 1), which is the focus of the jet, is a little higher and amounts to about 11 °C (TC 6) and 10 °C (TC 7). As the velocity plot has already

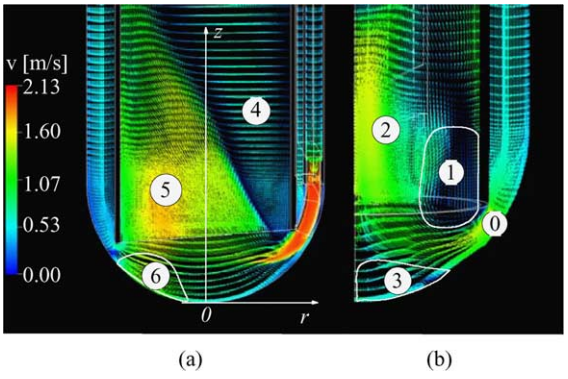

Fig. 3. Calculated velocity vectors in the (a) r–z-plane ($\phi = 0°$) and (b) r–z-plane ($\phi = 90°$). The corresponding dimensional velocity scale is depicted on the left side.

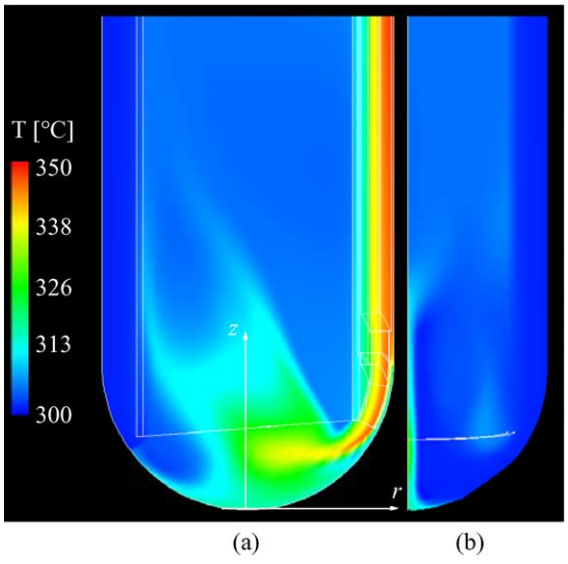

Fig. 4. Calculated temperature contours in the (a) r–z-plane ($\phi = 0°$) and (b) r–z-plane ($\phi = 90°$). The dimensional temperature scale is depicted on the left.

shown the jet is not strong enough to enter the opposite side of the annular gap, which is also reflected in the temperature distribution there. Nevertheless, a significant amount of the thermal energy of the jet is lost before it reaches the nozzle exit by the heat transport through the adjacent wall into the main flow of the annular gap. The recirculation area in the jet channel adjacent riser side at $\phi = 0°$ hardly experiences a temperature rise. Also, in the plane perpendicular $\phi = 0°$, namely $\phi = 90°$, the impact of the jet flow on the temperature distribution is weak, as Fig. 4(b) illustrates. Here, the jet is mainly concentrated in a small region of the symmetry plane of radius of about 50 mm. This rather local effect could mean in the MEGAPIE design that in case of miscellaneous beam positions local overheating can likely occur.

4. Comparison of experimental and numerical data

The experimental results discussed in this paragraph refer all to the defined reference case. Variations of the main flow rate or the jet flow rate are subject to the currently conducted experimental campaign, in order to exploit the different operational stages possible in MEGAPIE according to their pumps [9] and their cooling capability.

Fig. 5 shows the measured temperature distribution as a function of s along the lower hemisphere in a radius of $R = 84$ mm. As the jet exits the nozzle the adjacent TC(4) hardly experiences the hot jet, here mainly conduction takes place. As the flow proceeds the jet impinges upon the lower shell in positions which are depicted by higher temperatures there. Because most of the jet momentum is not directed to the center of the spherical shell, it rather turns before the center line and enters the core flow (see corresponding flow field in Fig. 3(a)), the temperature maximum is before the symmetry line. From this point, the temperature is continuously decreasing with growing s coordinate.

The jet itself does not penetrate to the opposite side so that the temperature there remains at the value of the inlet flow. A comparison of the numerical and experimental data shows a qualitatively good agreement in this flow domain. The difference in the nozzle outlet temperature originates from the limited computational flow domain, which predicts higher values in the simulation. The strong deviation at the position $s = 188$ mm arises from the fact that a stagnation point appears exactly there. For the numerical codes based on an averaging process like the k–ε or k–ω-turbulence model, these singularities can hardly be calculated exactly. Here, smallest deviations in the experiment or in the grid lead to significant deviations between experiment and numerical results.

Generally, the simulation underestimates the temperatures at the lower shell, except for the immediate vicinity of the jet nozzle ($s < 70$ mm). The temperature gradients found in the experiment are significantly larger than those predicted, which can not be explained by the omission of buoyancy effects in the simulation, they even would lead to smoother temperature gradients in the simulation. The remaining explanation for this deviation is that the flow field in this inertia governed part of the flow domain differs between numerical simulation and experiment. Here, water experiments simultaneously underway have to clarify this issue [10].

The measured temperature distribution in the thermocouple array in a height of $z = 105.7$ mm is displayed for the plane $\phi = 0°$ and in Fig. 6 and compared to the

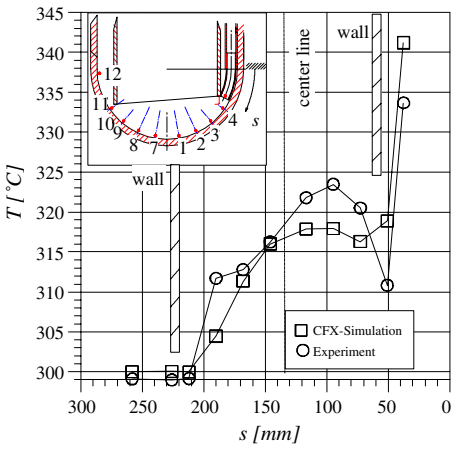

Fig. 5. Comparison of the measured and numerical data in the lower shell of the module as a function of s at the reference conditions.

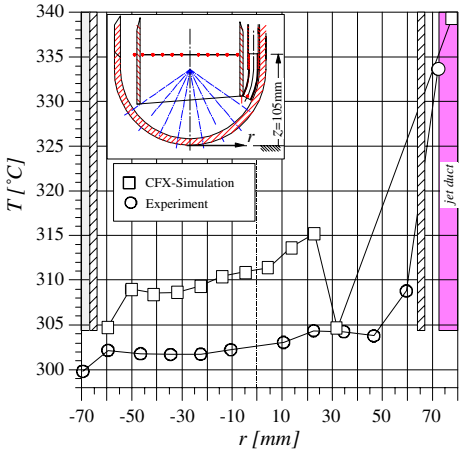

Fig. 6. Comparison of the measured and numerical data in the plane $z = 105.7$ mm ($\phi = 0°$) as a function of r at the reference conditions.

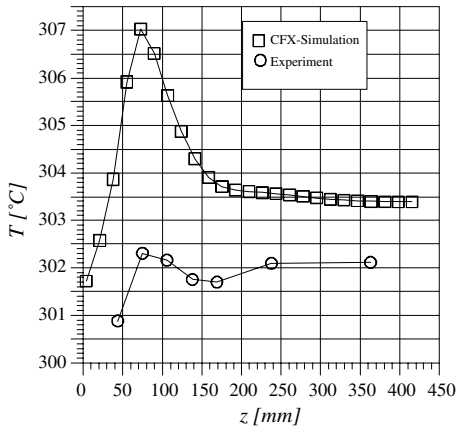

Fig. 7. Comparison of the measured and numerical data in the plane $r = -60$ mm ($\phi = 180°$) as a function of z at the reference conditions.

simulation. Here, qualitative differences between the two data sets appear. Especially the temperature at the jet duct adjacent wall is significantly lower in the experiment. One reason is again the limited flow domain in the simulation, which would lower the temperature in the mean by 7 °C. But, here another effect leads to the deviations. Here, buoyancy effects play a more significant role leading to a spreading of the temperature field and to a different velocity field in the riser tube than that calculated. Future studies have to clarify this.

Finally, in Fig. 7 the temperature is shown in a plane $r = -60$ mm = constant ($\phi = 180°$) as a function of the axial coordinate z. According to the measurements displayed in Fig. 7 the jet does not reach the opposite wall, because the temperatures measured there are significantly lower than the numerical predictions. Both differ qualitatively in shape and magnitude. The origin of this deviation may be caused by the reasons already named. However, for small z-values ($z < 50$ mm) the difference is already more than 1 °C, which is a strong indication for different flow fields between experiment and numerical simulation. Further parametric investigations in both experiments and simulation have to show, how sensitively the flow reacts to variations of the flow rate ratio and the supplied power.

5. Conclusions and outlook

Within this article we have presented a numerical and experimental study of the turbulent mixing a hot lead–bismuth jet into a cold main in a complex geometry similar to that of the lower part of the MEGAPIE beam window experiment. The discussion concentrates on one specific flow rate configuration of jet flow and main flow, which is in a similar range as it appears in MEGAPIE, namely $Q_{main} = 18$ m^3/h and $Q_{jet} = 1.2$ m^3/h.

In the technically most interesting part of the lower shell, where the jet flow is merging with the main flow exiting the annular downwards directed channel both simulation and experimental data reveal qualitatively and quantitatively reasonably good agreement. Minor deviations appear at the measurement positions, where stagnation points are located, which have to analyzed in more detail.

As the flow proceeds downstream, the turbulent mixing within the experiment is much more pronounced than the numerical simulation predict, which is expressed by significantly smaller measured temperatures. The general qualitative tendency of the energy decay within the fluid is captured by the simulation, however, the effective magnitude of the energy mixing process is underestimated. Therefore, a more detailed analysis by means of parametric studies in the experiment, e.g. flow rate ratio, heating power variations, are performed to quantify these deviations. Simultaneously on the numerical side sensitivity studies regarding the mesh, the influence of the turbulence model, the heat losses to the ambient, the heat conduction of the outer structure, the implementation of buoyancy and finally a more complete formulation of the geometry will be conducted.

Acknowledgments

This work bas been performed within the context of the EU-programs TECLA (FIKW-CT2000-00092) and MEGAPIE-TEST (FIS5-2001-00090) and is supported by the HGF Strategy Fund Project (01SF9926/3).

References

[1] B. Smith, Summary of the First CFD Benchmark Study. PSI-Internal Report *MPBE-4-BR-1/0*, 2002.
[2] J.A. Patorski, G.S. Bauer, I. Platnieks, Y. Takeda, 2000, Experimental estimation of optimum Bypass-jet-flow conditions for the cooling of the window of the SINQ liquid metal target, *PSI Report 2000, ISSN 1423-7350*, vol. VI, p. 42, PSI, CH-5232 Villigen, Switzerland.
[3] D.C. Wilcox, Multiscale model for turbulent flows; 24th Aerospace Science Meetings; American Institute of Aeronautics and Astronautics, 1986.
[4] W. Vieser, Th. Esch, F. Menter, CFX –5 Solver Theory; CFX. Didcot Oxfordshire OX11 OQR, United Kingdom, 2002.
[5] B.A. Kader, Int. J. Heat Mass Transfer 24 (9) (1981) 1541.
[6] V. Imbeni, C. Martini, S. Masini, G. Palombarini, The properties of the eutectic alloys Pb55.5Bi and Pb17Li, ENEA-Report DT-EUB-00001, Part 2, 1999.
[7] J.-U. Knebel, L. Krebs, U. Müller, B.P. Axcell, J. Fluid Mech. 368 (1998) 51.

[8] F. Ogino, H. Takeuchi, I. Kudo, T. Mizushina, Int. J. Heat Mass Transfer 23 (1980) 1581.
[9] R. Stieglitz, MHD-features of the Main service and Bypass pump in the MEGAPIE Design, FZKA Report-6826, 2003.
[10] J.-U. Knebel, X. Cheng, G. Grötzbach, R. Stieglitz, G. Müller, J. Konys, Thermalhydraulic and Material Specific Investigations into the Realization of an Accelerator Driven System (ADS) to Transmute Minor Actinides-Final Report. FZKA 6868, 2003.